

## Effects of Wide-Range $\gamma$ -Irradiation Doses on the Structures and Properties of 4,4'-Dicyclohexyl Methane Diisocyanate Based Poly(carbonate urethane)s

Chen Zhang,<sup>1</sup> Xiujuan Jiang,<sup>1</sup> Zhiyang Zhao,<sup>1</sup> Lixin Mao,<sup>1,2</sup> Liqun Zhang,<sup>1,2</sup> Phil Coates<sup>3</sup>

<sup>1</sup>Key Laboratory of Beijing City for the Preparation and Processing of Novel Polymer Materials, Beijing University of Chemical Technology, Beijing 100029, People's Republic of China

<sup>2</sup>State Key Laboratory of Organic-Inorganic Composites, Beijing University of Chemical Technology, Beijing 100029, People's Republic of China

<sup>3</sup>School of Engineering, Design, and Technology, Bradford University, BD7 1DP, United Kingdom

Correspondence to: L. Zhang (E-mail: zhanglq@mail.buct.edu.cn)

For medical applications, 4,4'-dicyclohexyl methane diisocyanate (HMDI)-based poly(carbonate urethane)s were synthesized from HMDI and 1,4-butanediol as hard segments and poly(carbonate diol) (number-average molecular weight = 2000 g/mol) as soft segments. The effects of wide-range  $\gamma$  irradiation on the samples were examined through a series of analytical techniques. Scanning electron microscopy revealed that  $\gamma$  irradiation etched and roughened the surfaces of the irradiated samples. The gel content and crosslinking density measurements confirmed that crosslinking occurred along with degradation at all of the investigated irradiation doses and the degree of both crosslinking and degradation increased with increasing irradiation dose. Fourier transform infrared spectroscopy demonstrated that chain scission in the  $\gamma$ -irradiated samples occurred at the carbonate and urethane bonds. The decreasing molecular weight and tensile strength indicated that the degradation increased with the  $\gamma$ -irradiation dose. Differential scanning calorimetry and dynamic mechanical thermal analysis indicated that  $\gamma$  irradiation had no significant effect on the phase-separation structures. There was a slight reduction in the contact angle. An evaluation of the cytotoxicity demonstrated the nontoxicity of the nonirradiated and irradiated polyurethanes. © 2014 Wiley Periodicals, Inc. *J. Appl. Polym. Sci.* **2014**, *131*, 41049.

**KEYWORDS:** biomedical applications; crosslinking; degradation; irradiation; polyurethanes

Received 26 February 2014; accepted 19 May 2014

**DOI:** 10.1002/app.41049

### INTRODUCTION

Polyurethane is considered to be a polymer with growing applications in medicine because of its combination of excellent oxidative biostability, biocompatibility, processability, and mechanical properties, such as abrasion resistance, toughness, flexibility, durability, and tensile strength.<sup>1</sup> Some of these properties are due to the segmented structure of polyurethane with hard segments (diisocyanate and chain extender) and soft segments [polyether, polyester, and poly(carbonate diol) (PCDL)]. However, implant devices that contain soft segments such as polyether and polyester significantly degrade *in vivo* after exposure to long-term biological environments because of hydrolytic or oxidative mechanisms.<sup>2–4</sup> Poly(ester urethane)s are no longer used for devices that are required for long-term implantation because of their poor hydrolytic stability. Poly(ether urethane)s will undergo oxidative degradation in several forms, including auto-oxidation, environmental stress cracking, and metal-ion

oxidation in the *in vivo* environment.<sup>5,6</sup> Because they have shown decreased susceptibility to oxidation, PCDLs have become the optimal choice as soft segments for long-term implantation.<sup>7,8</sup> However, poly(carbonate urethane)s are also subject to hydrolytic degradation *in vivo* like poly(ester urethane)s. Labow et al.<sup>9</sup> used an activated human monocyte-derived macrophage (MDM) cell system to assess the biostability of polycarbonate-based polyurethanes; the results showed that polycarbonate-based polyurethanes were susceptible to hydrolysis induced by MDM cells. Increasing the content of hard segments and the crystallinity of soft segments can improve the hydrolytic stability of poly(carbonate urethane)s.<sup>10,11</sup> Špírková<sup>12</sup> reported the composition–property relationship of novel all-aliphatic polycarbonate-based polyurethane elastomers. It was found that they had very attractive mechanical properties (e.g., an elongation at break between 600 and 800%), which was due to a distinctly segmented structure and strong physical rubbery

networks. Above all, the hard segments had a significant impact on the stability and biocompatibility. Recent work has indicated that aromatic polyurethanes based on toluene diisocyanate and 4,4'-methylene bis(phenyl isocyanate) (MDI) produced highly toxic aromatic amines during thermal and thermohydrolytic degradation.<sup>13–15</sup> Although similar to MDI, aliphatic 4,4'-dicyclohexylmethane diisocyanate (HMDI) can improve biosafety greatly without the release of toxic aromatic amines. Kuta<sup>16</sup> prepared polyurethane materials with HMDI, 1,4-butanediol, and a macrodiol (PCDL, polyoxypropylene diol, or polybutadiene diol). The research focused on the influence of the macrodiol type on the mechanical properties of polyurethane materials. Recently, we synthesized poly(carbonate urethane) elastomers with HMDI, 1,4-butanediol, and PCDL. The study was on the effect of the hard-segment contents on the relationship between the microphase-separation structure and properties.<sup>17</sup>

$\gamma$  irradiation has been widely used for the sterilization and surface modification of medical-grade polyurethanes. This material used in implanted medical devices must be critically sterilized before use. In general, sterilization by the use of steam or chemicals could have unfavorable effects, such as material degradation and cytotoxic action, on medical-grade polymers.<sup>18</sup> In recent years, high-energy irradiation, such as UV irradiation, electron beam radiation, and  $\gamma$  irradiation, have been found to be suitable for sterilization in biomedical applications. When polyurethane is exposed to UV irradiation, there is a deterioration of its crystallinity. UV irradiation can induce crazing of the surface and discoloration. The changes are due to the reactions taking place in the backbone of the polyurethane structure.<sup>19,20</sup> An effective industrial method for the sterilization of medical products is the use of  $\gamma$  irradiation.<sup>21,22</sup> This method is advantageous because  $\gamma$  irradiation not only has a strong ability to penetrate materials but is also economically feasible for the large-scale sterilization of products in sealed packages.<sup>18,23</sup> In addition to killing bacteria,  $\gamma$  irradiation may produce changes in the bulk polymer; this results in the formation of additional polar groups on the surface, which seems to increase the hydrophilicity and adhesion of cells to the polymer matrix. This effect on the surface significantly improves the biocompatibility of polyurethane contacted with tissues.<sup>24</sup>

Polyurethane has good resistance to low  $\gamma$ -irradiation doses; however, extremely high irradiation doses can alter its structure and properties and result in oxidation, chain scission, and crosslinking.<sup>25</sup> Previous studies have shown the effect of  $\gamma$  irradiation on the structure and properties of poly(ester urethane)s and poly(ether urethane)s in the range of sterilization doses. In general, aromatic polymers are more resistant to high-energy irradiation than aliphatic polymers, whereas the presence of impurities and additives may enhance degradation and/or crosslinking.<sup>26,27</sup> Gorna and Gogolewski<sup>28</sup> reported that when exposed to  $\gamma$  irradiation at a standard dose of 25 kGy, which was used for the sterilization of medical devices, experimental biodegradable poly(ester urethane)s and poly(ether urethane)s with different ratios of hydrophilic to hydrophobic contents underwent significant degradation; this was accompanied by reductions in the tensile strength and modulus. Przybytniak

et al.<sup>24</sup> reported the influence of  $\gamma$ -irradiation sterilization on poly(ester urethane)s designed for medical applications. The results confirm that the urethane segments were more resistant to ionizing irradiation than the soft segments and the presence of ester units facilitated the generation of free radicals. Haugen et al.<sup>29</sup> reported the effect of  $\gamma$ -irradiation dose on the cytotoxicity and material properties of poly(ether urethane)s. It was recommended that thermoplastic polyether–urethane should be sterilized by  $\gamma$  irradiation at a dose of 25 kGy or higher.

In this study, we synthesized poly(carbonate urethane)s from HMDI, PCDL [number-average molecular weight ( $M_n$ ) = 2000 g/mol], and 1,4-butanediol. In previous works, HMDI-based poly(carbonate urethane)s were less reported and showed potential biomedical value. There was little information in the literature on the identification of the effect of the  $\gamma$ -irradiation dose on the structures and properties of these unique poly(carbonate urethane)s in a wide range from 50 to 200 kGy. Scanning electron microscopy (SEM) was performed on the nonirradiated and irradiated samples to identify the changes in the surface morphology. A crosslinking density test, a gel content test, and gel permeation chromatography (GPC) were used to investigate the degree of degradation and crosslinking. Fourier transform infrared (FTIR) spectroscopy revealed the basic crosslinking and degradation kinetics of the irradiated samples. An array of characterization techniques, including tensile testing, differential scanning calorimetry (DSC), dynamic frequency sweeps, and cytotoxicity testing were used to quantify the effects of  $\gamma$  irradiation on the properties of the samples. In addition, a contact angle test was carried out to distinguish the effects of  $\gamma$  irradiation on the hydrophilic properties.

## EXPERIMENTAL

### Preparation of Polyurethane

The synthesis was carried out by a two-step reaction. In the first step, a prepolymer was obtained by the reaction of HMDI (Bayer, German) with PCDL (Asahi Kasei,  $M_n$  = 2000 g/mol). The reaction was carried out at 60–80°C for 2–2.5 h. In the second step, 1,4-butanediol was added to produce a final 1.05 ratio of NCO to OH groups. The catalyst was a bismuth catalyst (BiCAT8118). We processed the final polymer melt into sheet materials by casting it into a mold and curing it at 100°C for 24 h. The cured samples were stored for at least 1 week before use.

### $\gamma$ Irradiation

The cast-molded polymer samples were irradiated at doses of 50, 100, and 200 kGy from a <sup>60</sup>Co  $\gamma$  source at room temperature. Neither a vacuum nor protection with inert gas was applied.

### Material Characterization

**SEM.** The surface morphology of the polyurethane films was observed with a field emission scanning electron microscope (S-4700, Hitachi, Japan) in high-vacuum mode at an acceleration voltage of 10 kV. The average film thickness was 2 mm. All test specimens were vacuum-plated with gold for electrical conduction.

**Gel Content and Crosslinking Density Measurements.** After  $\gamma$  irradiation, the product (weight  $W_1$ ) containing sol and gel components was separated with the Soxhlet extraction method with  $\text{CH}_2\text{Cl}_2$  as the solvent for 72 h. The  $\text{CH}_2\text{Cl}_2$  solution containing the sol component and the insoluble product containing the gel component were dried *in vacuo* at room temperature until a constant weight was reached. The weight of the gel component was designated as  $W_2$ . The gel fraction was calculated by eq. (1):

$$\text{Gel content} = (W_2/W_1) \times 100\% \quad (1)$$

The crosslinking density of the gel was measured by the swelling technique with 1,4-dioxane as the solvent. Small pieces of samples were immersed in 1,4-dioxane for 72 h at 30°C. The swollen sample was wiped and weighed immediately. The crosslinking density was calculated with the Flory–Rehner equation.<sup>30</sup> The Flory interaction parameter ( $\chi$ ) for polyurethane extracted to 1,4-dioxane and the volume fraction of the polymer in the swollen state ( $v_{pm}$ ) were calculated according to eqs. (2) and (3):

$$\chi = B + (v_s/RT)(\delta_p - \delta_s)^2 \quad (2)$$

$$v_{pm} = \left\{ \left( m_0/\rho_p \right) / \left[ m_0/\rho_p + (m' - m_0) \right] \rho_s \right\} \times 100\% \quad (3)$$

where the modified coefficient  $B$  is 0.34 for the good solvent;  $R$  is the gas constant and  $T$  is the absolute temperature;  $\delta_p$  and  $\delta_s$  are the solubility parameters of the polymer and solvent, respectively;  $m'$  is the weight of the swollen gel;  $m_0$  is the initial weight of the polymer;  $\rho_p$  is the density of the polymer;  $\rho_s$  is the density of the solvent; and  $v_s$  is the molar volume of the solvent.

The molecular weights of the network chains were obtained from the Flory–Rehner relation according to eq. (4):

$$M_c = -V_s \rho_p \left( V_{pm}^{\frac{1}{3}} - V_{pm} / 2 \right) / \left[ \ln(1 - V_{pm}) + V_{pm} + \chi V_{pm}^2 \right] \quad (4)$$

where  $M_c$  is the average molecular weight of the chains between adjacent crosslinks.

**GPC.** GPC analyses were performed on a Waters150-C GPC system. All GPC analyses were carried out at a constant column temperature of 40°C. The carrier solvent was tetrahydrofuran (THF), and the carrier flow rate was 1 mL/min. Each polyurethane sample was prepared as a 4 mg/mL solution in spectroscopy-grade THF and injected into the GPC system. Triplicate analyses were performed for each polyurethane system.

**FTIR.** IR spectra of the polyurethanes were obtained with an FTIR spectrometer (Tensor 27, Bruker Optik, Germany) with an incorporated universal attenuated total reflection (ATR) sampling accessory. The average thickness used for measurements was 2 mm as obtained from tensile specimens. The wavelength range was from 4000 to 600  $\text{cm}^{-1}$  with a resolution of 4  $\text{cm}^{-1}$  and 32 scans. Spectra were obtained from five different samples. All spectra were baseline-corrected.

**Mechanical Properties.** Tensile testing was performed with a CMT4104 electronic tensile tester (SANS, China) according to Chinese Standards GB/T528-1998 and GB/T529-1999 at a cross-head speed of 500 mm/min. The dumbbell-shaped samples ( $25 \times 6 \times 2 \text{ mm}^3$ ) were prepared according to ISO/DIS 37-1990. For each measurement, the average and standard deviation of five replicate samples were taken.

A compression set under constant deflection in air was measured according to ASTM D 395-2003. The specimens were compressed by 25% for 72 h at 70°C. The compression set was taken as the percentage of the original deflection after the material was allowed to recover under standard conditions for 30 min. The compression set ( $C_B$ ) was calculated by eq. (5):

$$C_B = [(t_0 - t_i)/(t_0 - t_n)] \times 100\% \quad (5)$$

where  $t_0$  is the original specimen thickness,  $t_i$  is the specimen thickness after testing, and  $t_n$  is the spacer thickness

**Thermal Analysis.** DSC analysis was performed on a STARE system DSC1 instrument (Mettler-Toledo International, Inc., Switzerland). Volatiles were removed from the purging head with nitrogen at a rate of 50 mL/min. The weight of samples was 4–6 mg. The first run was heated from 25 up to 200°C at a rate of 10°C/min; it remained in this mode for 5 min and was then cooled to -100°C at a rate of -40°C/min. The second run was heated from -100 up to 200°C at a rate of 10°C/min. Two scans were performed on each sample. The first scan was used to remove the thermal history, and the second scan was used to record the results. Liquid nitrogen was used to bring the test cell to a low temperature. After each scan, the thermal transitions were analyzed to determine the glass-transition temperature.

**Dynamic Mechanical Analysis.** The storage modulus ( $E'$ ) and  $\tan \delta$  values of the polyurethane samples were measured on a DMAVA3000 dynamic mechanical analyzer (01 dB Co., Ltd., France). The measurements were made in tension mode at a strain amplitude of 0.1%. The temperature dependence of  $E'$  and the loss factor ( $\tan \delta$ ) were measured in the range -80 to 100°C at a frequency of 1 Hz and a heating rate of 3°C/min. Each sample was 15 mm long, 15 mm wide, and 2 mm thick.

**Contact Angle Measurements.** Contact angles were measured on an OCA15EC machine (Data-Physics, Germany) at ambient temperature. The water drops were dropped carefully onto the samples. Three samples of each material were measured, and three measurements were carried out for each sample. The average value of measurements performed at different positions on the same sample was taken as the contact angle.

**Cytotoxicity.** The 3-(4,5-dimethylthiazol-2-yl)-2,5-diphenyltetrazolium bromide (MTT; a tetrazole) colorimetric method was used for the cytotoxicity tests *in vitro* according to Chinese standard GB 16886.5-2003.

#### Statistics

Data were expressed as means with the standard deviation. Statistical analyses were performed by a one-way analysis of variance with SPSS software. Comparisons between the two groups were assessed by a Student  $t$  test. Statistical significance was considered to exist at  $p < 0.05$ .

## RESULTS AND DISCUSSION

### SEM

In this study, nonirradiated and irradiated samples were tested to identify changes induced by  $\gamma$  irradiation, as shown in Figure 1. The method involved testing the surface of the nonirradiated (at



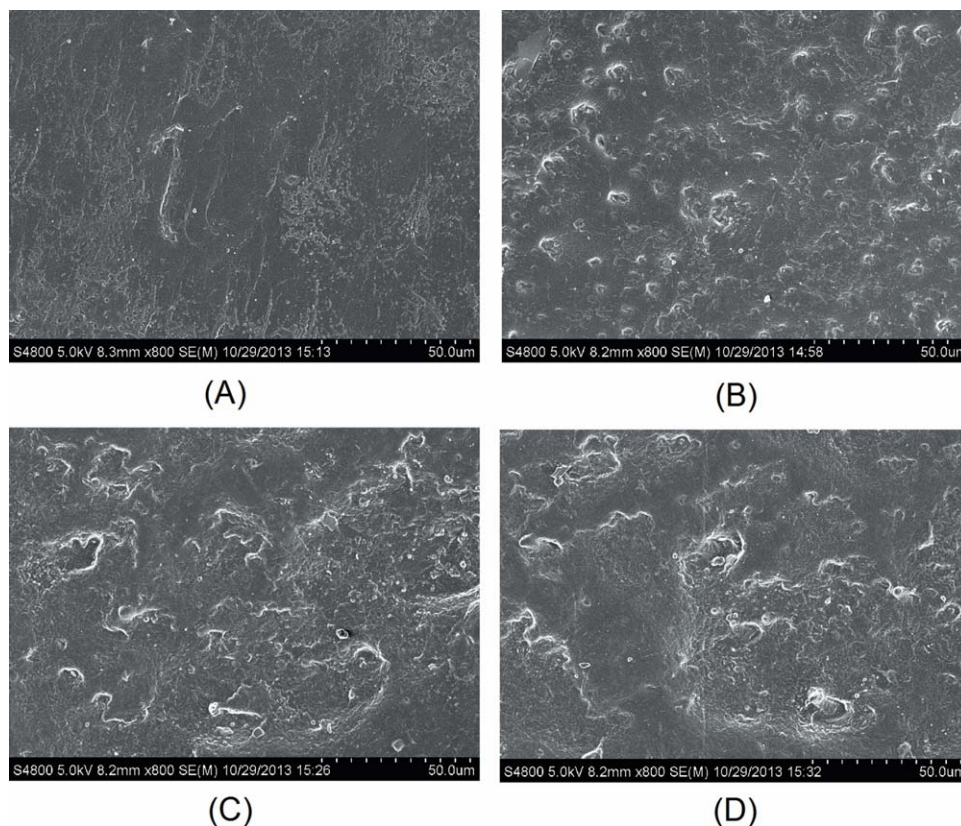


**Figure 1.** SEM micrographs of polyurethane samples before and after  $\gamma$  irradiation: (A) nonirradiated sample and samples irradiated with (B) 50, (C) 100, and (D) 200 kGy. [Color figure can be viewed in the online issue, which is available at [wileyonlinelibrary.com](http://wileyonlinelibrary.com).]

0 kGy) and  $\gamma$ -irradiated (at 50, 100, and 200 kGy) tensile specimens with SEM at a magnification of 800 $\times$ . As shown in Figure 1, the nonirradiated sample had an intact surface. However,  $\gamma$  irradiation could etch and roughen the surfaces of the irradiated samples. Even numerous small voids started to appear on the surface of the sample irradiated at a dose of 50 kGy; this showed that the surface exposed to  $\gamma$  irradiation underwent significant oxidation and degradation. The void radius remained nearly homogeneous at 5  $\mu\text{m}$ . With increasing irradiation dose, small voids gradually increased and expanded together. The surface of the irradiated materials was etched, and the roughness increased greatly. In addition, several voids of the samples irradiated at 100 and 200 kGy were larger and deeper than the voids of the samples irradiated at 50 kGy.

**Table I.** Gel Contents and Crosslinking Densities of the Nonirradiated and Irradiated Samples

Sample	Gel content (%)	$v_{pm}$ (%)	$M_c \times 10^3$ (g/mol)	$N_c \times 10^{-4}$ (mol/g)
0 kGy	0	0	0	0
50 kGy	52.8 $\pm$ 1.1	17.6 $\pm$ 0.5	7.25 $\pm$ 0.43	1.38 $\pm$ 0.03
100 kGy	48.6 $\pm$ 0.9	14.3 $\pm$ 0.4	11.29 $\pm$ 0.64	0.89 $\pm$ 0.05
200 kGy	40.8 $\pm$ 1.3	19.0 $\pm$ 0.2	6.13 $\pm$ 0.14	1.63 $\pm$ 0.04

#### Gel Content and Crosslinking Density Measurement

The gel content and crosslinking density of the nonirradiated and irradiated polyurethane samples were presented in Table I.  $N_c$  is the inverse of  $M_c$ . The sample irradiated at 0 kGy was completely dissolved after it was swollen in  $\text{CH}_2\text{Cl}_2$  for 72 h. It was observed that the irradiated samples did not completely dissolve after they were extracted in  $\text{CH}_2\text{Cl}_2$  for 72 h. At the same time, the decrease in the gel content was almost 25% from 50 to 200 kGy; this indicated that degradation occurred at all of the investigated irradiation doses and the degree of degradation increased with increasing irradiation dose. For the samples irradiated at 200 kGy, more degradation led to lower gel contents than for the samples irradiated at 50 kGy. In addition,  $M_c$  increased between 50 and 100 kGy; then, it decreased. One would expect the crosslinking density to increase with the dose. Hence, we concluded that crosslinking occurred along with degradation at all of the investigated irradiation doses.

The photographs of the nonirradiated and irradiated samples are shown in Figure 2, which indicates the ability of the irradiated samples to maintain their original shapes after they were swollen in  $\text{CH}_2\text{Cl}_2$  for 72 h. When the solvent was removed, the irradiated sample was put on filter paper and quickly photographed. The sample irradiated at 50 kGy had significant swelling compared to its original shape. The sample irradiated at 200 kGy had the strongest ability to maintain its original shape. The larger the shape change was, the lower the crosslinking

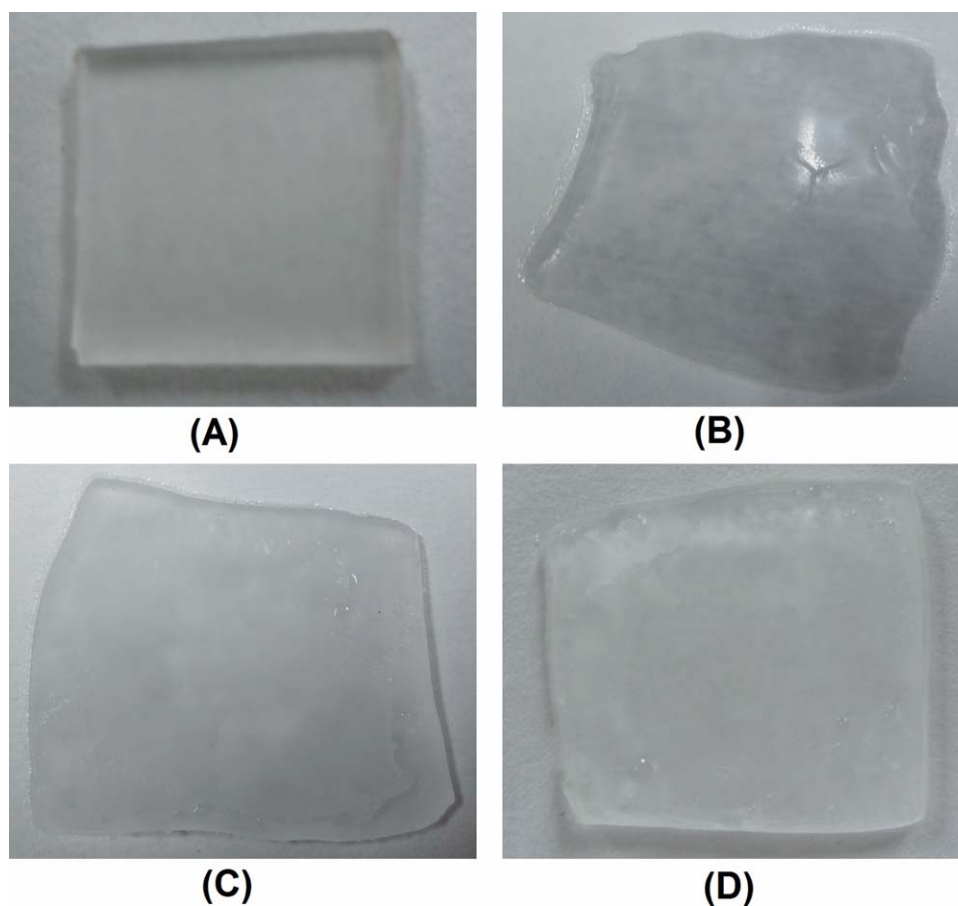


**Figure 2.** Photographs of the nonirradiated samples and irradiated samples after swelling in  $\text{CH}_2\text{Cl}_2$  for 72 h: (A) nonirradiated sample and samples irradiated with (B) 50, (C) 100, and (D) 200 kGy. [Color figure can be viewed in the online issue, which is available at [wileyonlinelibrary.com](http://wileyonlinelibrary.com).]

density of the gel was. The photographs were consistent with the results of the crosslinking density measurement.

### GPC

The GPC results represent the changes in the molecular weights in the sol fractions.  $\gamma$  irradiation caused a substantial degradation of the samples, as shown in Table II, with a decrease in  $M_n$ , viscosity-average molecular weight ( $M_v$ ), weight-average molecular weight ( $M_w$ ), and polydispersity index (PDI) with increasing irradiation dose. The reduction in  $M_n$  of the samples irradiated at 50 and 100 kGy were 15.5 and 27.5%, respectively. A large drop (51.1%) in  $M_n$  occurred at 200 kGy and was accompanied by a slight reduction (15.8%) in PDI. In conclusion, the degree of degradation increased with increasing irradiation dose. Above all, an anomalous increase in PDI at 100 kGy occurred; this may have been due to the lower molecular weight segments that resulted

from degradation. The phenomenon was consistent with the increase in  $M_c$  at 100 kGy, as shown in Table I.

### FTIR Spectroscopy

To quantitatively evaluate the changes in the chemical structures of the irradiated polyurethane samples, the ratios between the areas of specific absorption bands in the IR spectra were calculated. Figure 3 presents the spectra obtained for the nonirradiated and irradiated polyurethane samples. The corresponding ratios between the areas of specific absorption bands are given in Table III.

In the IR spectra, there were no evident changes in the absorbance band positions. However, the results given in Table III show that  $\gamma$  irradiation actually induced changes in the chemical structures of the irradiated samples. The ratio of the area of the band at  $3326\text{ cm}^{-1}$  to that of the band at  $2934\text{ cm}^{-1}$  showed

**Table II.** Molecular Weights of the Polyurethanes Before and After  $\gamma$  Irradiation

Sample	$M_n$	$M_v$	$M_w$	PDI
0 kGy	$119,868 \pm 3447$	$208,800 \pm 2707$	$230,000 \pm 3798$	$1.9 \pm 0.04$
50 kGy	$101,250 \pm 1212$	$163,000 \pm 2414$	$179,400 \pm 2568$	$1.8 \pm 0.02$
100 kGy	$86,890 \pm 1131$	$154,000 \pm 1978$	$173,700 \pm 2403$	$2.0 \pm 0.05$
200 kGy	$58,578 \pm 715$	$89,600 \pm 1783$	$95,900 \pm 1481$	$1.6 \pm 0.05$

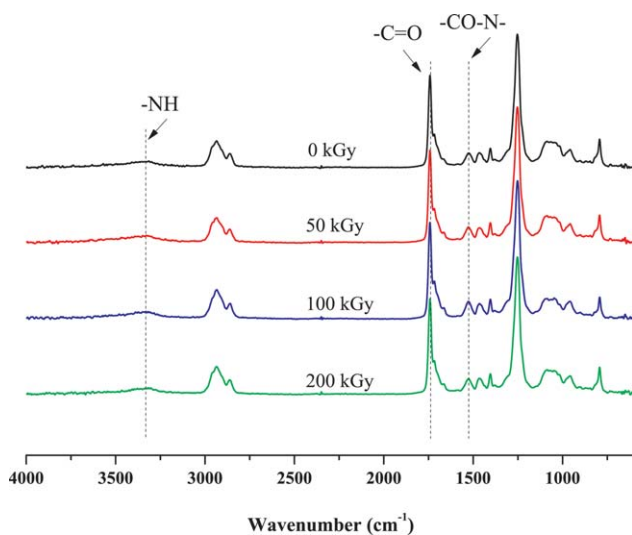


**Figure 3.** ATR-IR spectra for the nonirradiated and irradiated polyurethane samples. [Color figure can be viewed in the online issue, which is available at [wileyonlinelibrary.com](http://wileyonlinelibrary.com).]

an appreciable decrease at an irradiation dose of 200 kGy. Because these bands were related to N—H stretching, a decrease in this ratio indicated a substantial loss and degradation of urethane groups at high irradiation doses. The degradation was because C=O in the  $\alpha$  position of NH was oxidized, as reported by Shintani and Nakamura.<sup>31</sup> Most importantly, the ratio of the area of the absorption band at  $1741\text{ cm}^{-1}$  to that of the absorption band at  $1464\text{ cm}^{-1}$  showed a slight decrease at 200 kGy. These bands were related to the stretching of non-hydrogen-bonded C=O in both the urethane and the carbonate groups. A decrease in this ratio indicated the oxidation of the methylene groups in the  $\alpha$  position of the carbonate groups. The last products were aldehydes and carboxylic acids.<sup>32</sup> A decrease in the concentration of C—N around  $1525$  to  $1464\text{ cm}^{-1}$  suggested the degradation of the urethane groups as a result of the scission of C—N bonds. The stretching vibrations of C—O—C, represented by the ratio of the area of the band at  $1091\text{ cm}^{-1}$  to that of the band at  $1464\text{ cm}^{-1}$ , decreased at all of the investigated  $\gamma$ -irradiation doses, probably because of the scission of the C—O bonds in the carbonate groups. The ratio of the area of the band at  $957\text{ cm}^{-1}$  to that of the band at  $1464\text{ cm}^{-1}$ , represent-

ing the concentration of carbonate groups in the soft segments, also decreased at all of the investigated irradiation doses; this indicated that the scission of soft segments in the  $\gamma$ -irradiated samples mainly occurred at the carbonate bonds.

In summary,  $\gamma$  irradiation produced many changes in the HMDI-based poly(carbonate urethane)s in our study. We concluded that degradation occurred at all of the investigated irradiation doses. In addition, the degree of degradation increased with increasing  $\gamma$ -irradiation dose, especially at 200 kGy. Furthermore, the urethane groups were more resistant to  $\gamma$  irradiation compared with the carbonate groups at an irradiation dose of 200 kGy. We concluded that chain scission in the hard segments proceeded via the oxidation of C=O in the  $\alpha$  position of NH and the scission of the C—N bonds. Chain scission in soft segments occurred via the oxidation of the methylene groups in the  $\alpha$  position of the carbonate groups and the scission of the C—O bonds. The possible degradation reactions are presented in Scheme 1.

Both the results of the gel content and crosslinking density showed that crosslinking existed at 50 kGy. Murray et al.<sup>33</sup> provided a mechanism for crosslinking in irradiated poly(ether urethane)s. First, the methylene groups in the  $\alpha$  position of the urethane and carbonate groups were oxidized and generated free radicals. Second, free radicals combined together to form C—C bonds. Shintani and Nakamura<sup>31</sup> proposed that a mechanism of crosslinking occurred in  $\gamma$ -irradiated polyurethane with *p,p'*-methylenediphenyl diisocyanate/1,4-butanediol as hard segments. First, one secondary amino group in the urethane bonds lost a hydrogen radical. Second, nitrogen radicals combined to form tertiary amino groups.

On the basis of the previous mechanisms and the structural similarities of the materials involved, we proposed a possible mechanism for the crosslinking of HMDI-based poly(carbonate urethane)s (see Scheme 2).

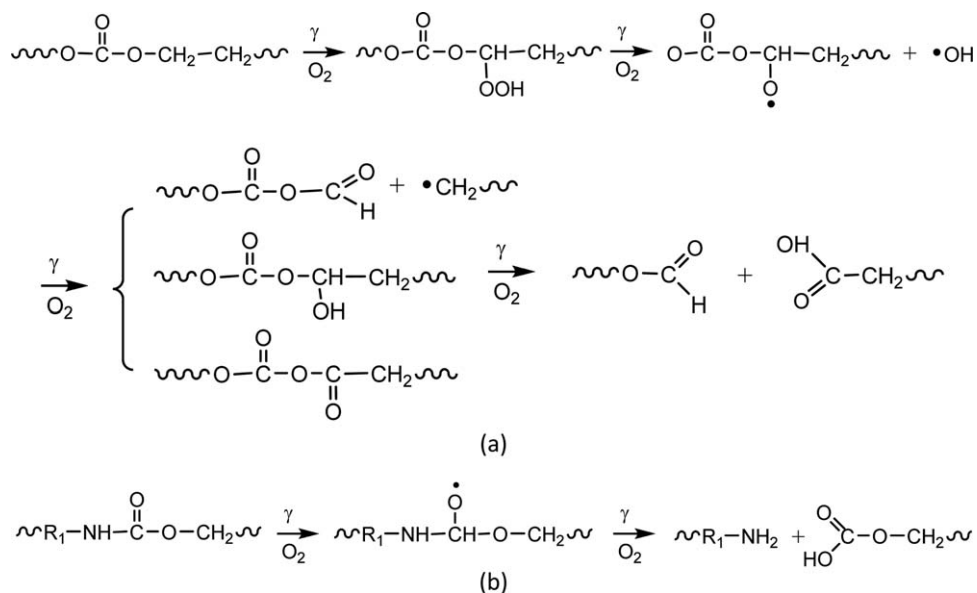
### Mechanical Properties

As shown in Figure 4, with increasing doses of  $\gamma$  irradiation, the tensile strength decreased, whereas the elongation at break and modulus at 100% elongation increased. Table IV shows the tensile strength, elongation at break, modulus at 100% elongation, hardness, and compression set of polyurethane samples at different irradiation doses. Table IV shows that the

**Table III.** ATR-IR Results for the Polyurethanes Before and After  $\gamma$  Irradiation

Sample	Ratio				
	1	2	3	4	5
0 kGy	1.302	6.66	1.189	1.886	1.586
50 kGy	1.439	6.84	1.178	1.768	1.482
100 kGy	1.343	6.65	1.171	1.262	1.537
200 kGy	1.273	6.58	1.178	1.623	1.584

Ratios between the areas of specific absorption bands are shown: (1)  $3326\text{ cm}^{-1}$  (—NH—)/ $2934\text{ cm}^{-1}$  (—CH<sub>2</sub>—), (2)  $1741\text{ cm}^{-1}$  (C=O)/ $1464\text{ cm}^{-1}$  (—CH<sub>2</sub>—), (3)  $1525\text{ cm}^{-1}$  (—CO—N—)/ $1464\text{ cm}^{-1}$  (—CH<sub>2</sub>—), (4)  $1091\text{ cm}^{-1}$  (—C—O—C—)/ $1464\text{ cm}^{-1}$  (—CH<sub>2</sub>—), and (5)  $957\text{ cm}^{-1}$  (—O—C—O—)/ $1464\text{ cm}^{-1}$  (—CH<sub>2</sub>—).

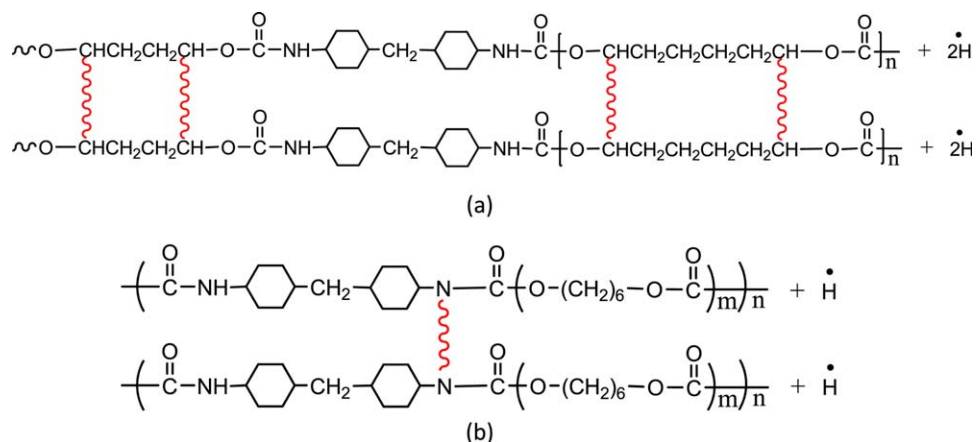


**Scheme 1.** Possible oxidation mechanism in irradiated polyurethane: (a) soft segments and (b) hard segments.

200-kGy sample had the lowest hardness and highest compression set; this was due to chain scission resulting from oxidation and degradation at high  $\gamma$ -irradiation doses. During the tensile process, the sol part comprised of broken chains by  $\gamma$  irradiation in polyurethane decreased the modulus, tensile strength, and compression set and increased the elongation at break through a quasi-plasticization effect. However, the crosslinking of polyurethane led by irradiation increased the modulus and restricted the deformation of macromolecular chains. These two mechanisms competed with each other and, therefore, resulted in such a regulation in mechanical performance. Overall, the mechanical properties of the HMDI-based poly(carbonate urethane)s could withstand multiple exposures up to a dose of 100 kGy. At the same time, we were also able to adjust the performance of polyurethane by the irradiation method.

#### Dynamic Mechanical Analysis

Dynamic mechanical thermal analysis (DMTA) testing was used to study the damping properties of the nonirradiated and irradiated samples. The temperature dependence of  $E'$  and  $\tan \delta$  are shown in Figure 5. In the  $\log E'$  versus temperature curves, it was obvious that all of the samples had a single-phase structure, as shown by the presence of only one relaxation in the region around  $0^\circ\text{C}$ ; this was attributed to the glass transition in the soft segments. On the whole, there were little changes in Figure 5 because the irradiation did not significantly alter the phase-separation structure. A detailed investigation of the  $\tan \delta$  curves showed that the peak of the glass-transition temperature at 200 kGy shifted slightly to a lower temperature; this was mainly attributed to the broken chains caused by  $\gamma$  irradiation. The value of  $\tan \delta$  at 200 kGy also slightly decreased compared with those at



**Scheme 2.** Possible mechanism of crosslinking in irradiated polyurethane: (a) soft segments and (b) hard segments. [Color figure can be viewed in the online issue, which is available at [wileyonlinelibrary.com](http://wileyonlinelibrary.com).]



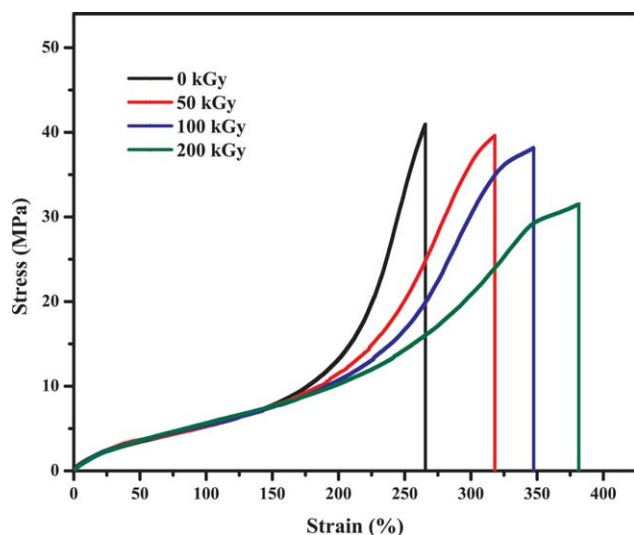


**Figure 4.** Tensile stress–strain curves for polyurethane samples with different doses of irradiation. [Color figure can be viewed in the online issue, which is available at [wileyonlinelibrary.com](http://wileyonlinelibrary.com).]

the other doses. This may have been caused by the crosslinking, which improved the elasticity and reduced the viscosity loss in the glass-transition region.

The structure of the nonirradiated samples was a self-assembly system. However, chain scission and crosslinking at 200 kGy changed the original good phase-separation structures. As a result,  $\tan \delta$  appeared to increase in the non-glass-transition region.

### Thermal Analysis

The phase-separation structure of the synthesized polyurethane samples was assessed with DSC. The DSC thermograms of the polyurethane samples with different doses of irradiation are shown in Figure 6. When all of the samples were heated to 200°C in the first scan, the hard and soft segments were completely dissociated and in a random coil state. Then, all of the samples were cooled at the same rate of  $-40^\circ\text{C}/\text{min}$ . In the cooling process, hard and soft segments were rearranged. Therefore, during the second scan, the samples had the same thermal history. As a result, the influence of different doses on the phase-separation structure were reflected truly by the second scan of the DSC curves. As shown in Figure 6, the glass transitions of the soft segments had slight variations in the temperature range from

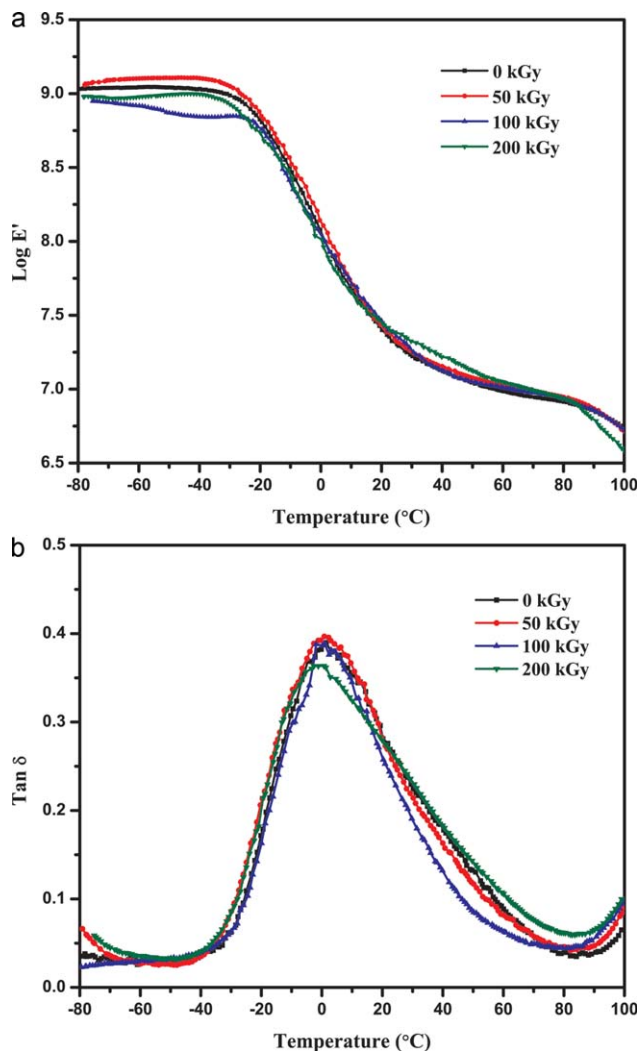


**Figure 5.** DMTA curves of the nonirradiated and irradiated samples: (a)  $\log E'$  and (b)  $\tan \delta$ . [Color figure can be viewed in the online issue, which is available at [wileyonlinelibrary.com](http://wileyonlinelibrary.com).]

$-28$  to  $-24^\circ\text{C}$ . These results were in agreement with the conclusions achieved by DMTA.

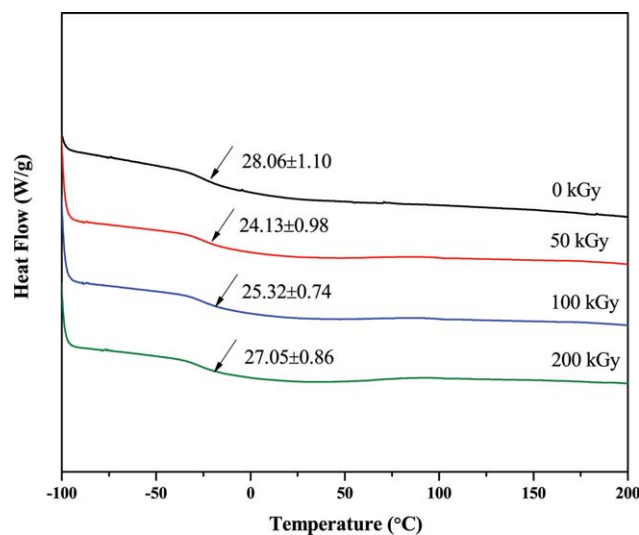
### Contact Angle Measurements

Figure 7 shows the contact angle of the polyurethane samples at different irradiation doses. A notable decrease in the contact angle could be seen between 50 and 100 kGy ( $p < 0.01$ ). A reduction in the contact angle was related to the surface degradation and/or oxidation (Scheme 1), which formed a low-

**Table IV.** Mechanical Properties of Polyurethane Samples with Different Doses of Irradiation

Sample	Tensile strength (MPa)	Elongation at break (%)	Modulus at 100% elongation (MPa)	Shore A hardness	Compression set (%)
0 kGy	$40.9 \pm 1.8$	$266 \pm 18$	$5.33 \pm 0.20$	$77 \pm 1$	$52 \pm 2$
50 kGy	$39.5 \pm 3.5$	$318 \pm 27$	$5.94 \pm 0.16$	$79 \pm 2$	$50 \pm 2$
100 kGy	$38.2 \pm 2.7$	$347 \pm 31$	$5.66 \pm 0.21$	$80 \pm 1$	$53 \pm 1$
200 kGy	$31.5 \pm 1.7$	$382 \pm 21$	$6.09 \pm 0.31$	$73 \pm 1$	$61 \pm 1$





**Figure 6.** DSC curves (second scan) for the nonirradiated and irradiated samples. [Color figure can be viewed in the online issue, which is available at [wileyonlinelibrary.com](http://wileyonlinelibrary.com).]

molecular-weight surfactant on the surface.<sup>28</sup> The reduction of the contact angle may have been consistent with the increase in  $-C=O$ ,  $-OH$ , and  $-NH_2$  hydrophilic functionalities on the surface.<sup>34</sup> These results suggest that  $\gamma$  irradiation enhanced the wetting capability of the polyurethane. An increase in the contact angle between 100 and 200 kGy could perhaps have been related to the complex microscopic–nanoscopic architecture of the surface, as shown in the SEM micrographs ( $p < 0.05$ ).

### Cytotoxicity

To assess the cytotoxicity of the polymeric materials for medical use, L-929 mouse fibroblasts were used to detect the relative cell proliferation rate of extracted liquid for polyurethane samples at different doses of irradiation by MTT assay. The results shown in Figure 8 indicate that the relative growth rate was high, and the cytotoxicity was 0 grade for 50 kGy and 1 grade

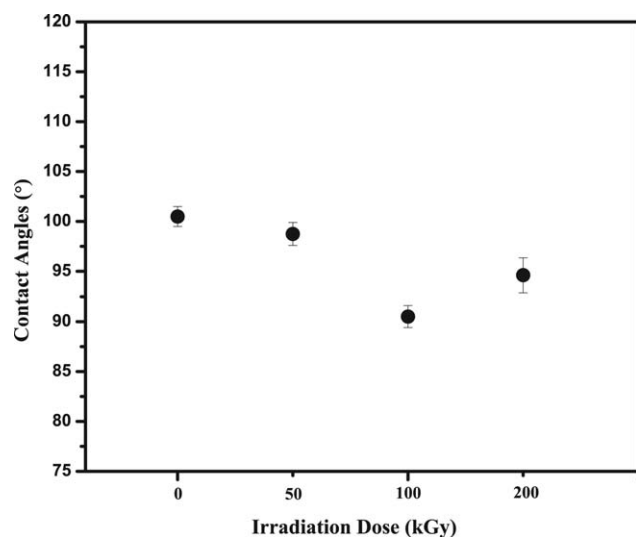


**Figure 7.** Effect of the irradiation dose on the contact angle of the polyurethane samples.

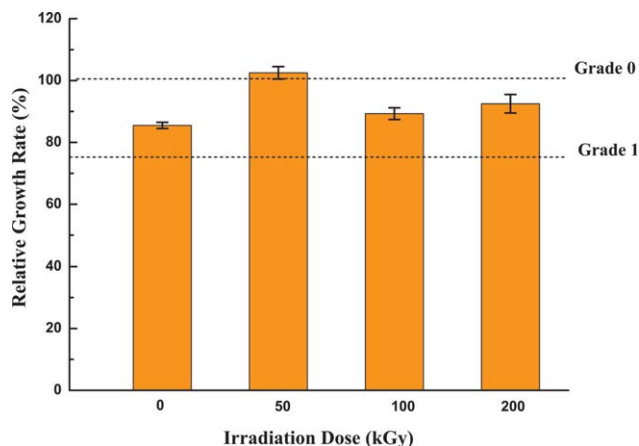


**Figure 8.** Cell relative growth rate of the extracted liquid for the polyurethane samples by the MTT assay. [Color figure can be viewed in the online issue, which is available at [wileyonlinelibrary.com](http://wileyonlinelibrary.com).]

for the other three samples according to the test standard of USP; this means that all of the nonirradiated and irradiated samples had no cytotoxicity. In addition, the samples treated with irradiation performed better than the nonirradiated sample in the cytotoxicity test ( $p < 0.05$ ). The phenomenon may have been due to the fact that the residual monomers were bonded back into the polymer structure by  $\gamma$  irradiation. In conclusion, the dose of irradiation used for the poly(carbonate urethane)s was safe and had no influence on the cytotoxicity of the polyurethane samples.

### CONCLUSIONS

The use of different doses of  $\gamma$  irradiation resulted in considerable modifications to the structures and properties of HMDI-based poly(carbonate urethane)s for medical use.

Four key areas of analysis, namely, surface morphology, chemical structure, properties, and biosafety, were used to identify the modifications led by irradiation. SEM showed that irradiation caused surface oxidation of the polyurethane materials, probably because of the radicals produced by radiolysis with oxygen. Surface oxidation also led to a reduction in the contact angle and improved the hydrophilic ability of the surface of the irradiated samples. The gel content and crosslinking density measurements led us to the conclusion that crosslinking occurred simultaneously with degradation at all of the investigated irradiation doses. The degrees of both crosslinking and degradation increased with increasing irradiation dose. FTIR spectroscopy demonstrated that chain scissions occurred mainly by carbonate and urethane bonds in the  $\gamma$ -irradiated samples. The decrease in the molecular weight and tensile strength of the irradiated samples suggested that the degree of degradation increased with increasing irradiation dose. Because the irradiation did not significantly alter the phase-separation structure, only slight changes occurred in the thermal and dynamic mechanical properties. Cytotoxicity evaluation demonstrated the nontoxicity of the nonirradiated and irradiated polyurethanes; this makes the HMDI-based poly(carbonate urethane)s promising for biomedical applications in the future.

## REFERENCES

1. Simmons, A.; Hyvarinen, J.; Odell, R. A.; Martin, D. J.; Gunatillake, P. A.; Noble, K. R. *Biomaterials* **2004**, *25*, 4887.
2. Boretos, J. W.; Detmer, D. E.; Donachy, J. H. *J. Biomed. Mater. Res.* **1971**, *5*, 373.
3. Wilson, D. J.; Rhodes, N. P.; Williams, R. L. *Biomaterials* **2003**, *24*, 5069.
4. El All, S. A. *J. Phys. D* **2007**, *40*, 6014.
5. Takahara, A.; Coury, A. J.; Hergenrother, R. W.; Cooper, S. L. *J. Biomed. Mater. Res.* **1991**, *25*, 341.
6. Santerre, J. P.; Labow, R. S.; Duguay, D. G.; Erfle, D.; Adams, G. A. *J. Biomed. Mater. Res.* **1994**, *28*, 1187.
7. Tanzi, M. C.; Mantovani, D.; Petrini, P.; Guidoin, R.; Laroche, G. *J. Biomed. Mater. Res.* **1997**, *36*, 550.
8. Seifalian, A. M.; Salacinski, H. J.; Tiwari, A.; Edwards, A.; Bowald, S.; Hamilton, G. *Biomaterials* **2003**, *24*, 2549.
9. Labow, R. S.; Meek, E.; Santerre, J. P. *Biomaterials* **2001**, *22*, 3025.
10. Christenson, E. M.; Dadsetan, M.; Wiggins, M.; Anderson, J. M.; Hiltner, A. *J. Biomed. Mater. Res.* **2001**, *56*, 516.
11. Tang, Y. W.; Labow, R. S.; Santerre, J. P. *J. Biomed. Mater. Res.* **2001**, *56*, 516.
12. Špírková, M.; Pavličević, J.; Strachota, A.; Poreba, R.; Berac, O.; Kaprálková, L.; Baldrian, J.; Šlouf, M.; Lazić, N.; Budinski-Simendić, J. *Eur. Polym. J.* **2011**, *47*, 959.
13. Shintani, H. *J. Anal. Toxicol.* **1991**, *15*, 198.
14. Shintani, H.; Nakamura, A. *J. Anal. Toxicol.* **1989**, *13*, 354.
15. Shintani, H. *Radiat. Phys. Chem.* **1996**, *47*, 139.
16. Kuta, A.; Hrdlička, Z.; Strachota, A.; Špírková, M. *Mater. Manuf. Processes* **2009**, *24*, 1214.
17. Jiang, X. J.; Shi, R.; Yu, C. K.; Chen, D. F.; Zhang, L. Q. *China Plast.* **2012**, *9*, 22.
18. Matthews, I. P.; Gibson, C.; Samuel, A. H. *Clin. Mater.* **1994**, *15*, 191.
19. Zia, K. M.; Barikani, M.; Bhatti, I. A.; Zuber, M.; Barmar, M. *Carbohydr. Polym.* **2009**, *77*, 54.
20. Zia, K. M.; Bhatti, I. A.; Barikani, M.; Zuber, M.; Sheikh, M. A. *Nucl. Instrum. Methods Phys. Res. Sect. B* **2009**, *267*, 1811.
21. Abraham, G. A.; Frontini, P. M.; Cuadrado, T. R. *J. Appl. Polym. Sci.* **1997**, *65*, 1193.
22. Alberto, R. B.; Rafacel, S.; Alejandro, M. M.; Perlro, A. *Contrib. Nephrol.* **2002**, *137*, 138.
23. Brinston, R. M.; Wilson, B. K. *Med. Device Technol.* **1993**, *4*, 18.
24. Przybytniak, G.; Kornacka, E.; Ryszkowska, J.; Bil, M.; Rafalski, A.; Woźniak, P.; Lewandowska-Szumieł, M. *Nukleonika* **2006**, *51*, 121.
25. Chapiro, A. *Nucl. Instrum. Methods Phys. Res. Sect. B* **1995**, *105*, 5.
26. Bruck, S. D. *J. Biomed. Mater. Res.* **1971**, *5*, 139.
27. Goldman, M.; Pruitt, L. *J. Biomed. Mater. Res.* **1998**, *40*, 378.
28. Gorna, K.; Gogolewski, S. *Polym. Degrad. Stab.* **2003**, *79*, 465.
29. Haugen, H. J.; Brunner, M.; Pellkofer, F.; Aigner, J.; Will, J.; Wintermantel, E. *J. Biomed. Mater. Res. B* **2007**, *80*, 415.
30. Flory, P. J.; Rehner, J. *J. Chem. Phys.* **1943**, *11*, 512.
31. Shintani, H.; Nakamura, A. *J. Appl. Polym. Sci.* **1991**, *42*, 1979.
32. Wilhelm, C.; Gardette, J. *Polymer* **1998**, *39*, 5973.
33. Murray, K. A.; Kennedy, J. E.; McEvoy, B. *Eur. Polym. J.* **2013**, *49*, 1782.
34. Mrad, O.; Saunier, J.; Aymes, C. C.; Rosilio, V.; Agnely, E.; Aubert, P. *Radiat. Phys. Chem.* **2010**, *79*, 93.